

# Epilayer Optimization of NPN SiGe HBT with n+ Buried Layer Compatible With Fully Depleted SOI CMOS Technology

Prasanna Kumar Misra and S. Qureshi

**Abstract**— In this paper, the epi layer of npn SOI HBT with n+ buried layer has been studied through Sentaurus process and device simulator. The doping value of the deposited epi layer has been varied for the npn HBT to achieve improved  $f_tBV_{CEO}$  product (397 GHzV). As the  $BV_{CEO}$  value is higher for low value of epi layer doping, higher supply voltage can be used to increase the  $f_t$  value of the HBT. At 1.8 V  $V_{CE}$ , the  $f_tBV_{CEO}$  product of HBT is 465.5 GHzV. Further, the film thickness of the epi layer of the SOI HBT has been scaled for better performance (426.8 GHzV  $f_tBV_{CEO}$  product at 1.2 V  $V_{CE}$ ). The addition of this HBT module to fully depleted SOI CMOS technology would provide better solution for realizing wireless circuits and systems for 60 GHz short range communication and 77 GHz automotive radar applications. This SOI HBT together with SOI CMOS has potential for future high performance SOI BiCMOS technology.

**Index Terms**— Fully depleted, sentaurus, SiGe HBT, SOI

## I. INTRODUCTION

The SiGe heterojunction bipolar transistors have been popular choice for high speed analog and RF circuit applications [1]. The working principle of HBTs and the review work are given in detail in [1-5]. Several works

have been reported on BiCMOS technology on bulk substrate that can be found from the literature [6-8]. Although BiCMOS technology on bulk substrate offers devices with promising performance, the process complexity, isolation among devices and power consumption have been the main issues in deep submicron lithography nodes. The emergence of SOI as an excellent platform for short channel MOSFETs has motivated researchers to design and optimize HBTs on thin film SOI. The detailed discussion on integration of SiGe HBT with CMOS on SOI can be found in [9, 10]. The advantages of this integration on SOI platform are also discussed in [11, 12].

A novel vertical bipolar transistor compatible with SOI CMOS was demonstrated in [13]. Recently, researchers have been trying to integrate the HBT with SOI CMOS to offer SOI BiCMOS technology [14-17]. The SOI CMOS technology has been of interest in the industry due to its scalability and reduced short channel effects. The HBTs that are compatible with the fully depleted SOI CMOS technology have poor performance in terms of speed due to the high value of collector resistance. Therefore, it is of interest to improve the performance of the SOI HBT. Recently, simulation study of SOI HBT with buried layer has been performed [18] and a high performance SOI HBT compatible with 130 nm SOI CMOS technology is proposed. Though SiGe HBT with buried silicide layer has been discussed in [19], the HBT is not compatible with advanced fully depleted SOI CMOS technology. A fully self aligned Si/SiGeC HBT with boron in-situ doped polybase, phosphorus doped emitter and nickel silicide has been reported in [20].

Using different device design approach researchers have explored performance improvement in HBT [18-21].

In this paper, 2D numerical simulation studies have been performed on SOI HBT compatible with fully depleted SOI CMOS which is in a way an extension of our previous work [18]. The SOI HBT is optimized for 65 nm technology node. The epilayer is optimized to achieve higher  $f_tBV_{CEO}$  product. The fabrication procedure and the operating principle of the HBT are discussed in section II. The dc and ac characteristics of SOI HBT have been discussed by varying the doping value of the epi layer. The optimal doping value obtained from the simulations is reported in section III. Section IV describes the scaling of epi layer thickness to obtain better performance. Finally the conclusion is given in section V.

## II. NPN SOI HBT WITH BURIED LAYER

The proposed SOI HBT with n+ buried layer of 0.15  $\mu\text{m}^2$  area is shown in Fig. 1. The fabrication of the device is given as follows. An SOI substrate is taken with 20 nm film thickness. By applying the rule of ETSOI ( $T_{si} = L_G/3$ ) [22], this substrate is fully depleted and is optimal for SOI CMOS technology with 65 nm node. The SOI film is doped with  $1 \times 10^{20} \text{ cm}^{-3}$  in the area where the HBT is to be fabricated. To achieve this doping value, a dose of  $8 \times 10^{14} \text{ cm}^{-2}$  is used at 30 KeV. A 100 nm n-type epi layer is deposited on the n+ buried layer. The rest of the fabrication procedure can be followed from [23] to fabricate the proposed npn SOI HBT. In the process simulations, phosphorus has been used for the n-type collector and the polysilicon emitter. The experimental HBTs use arsenic doped emitter [23, 24]. Boron is used in the base. After the epitaxial growth of SiGe base layer, 12 nm of silicon cap layer has been used for the emitter diffusion. The process steps reported for the experimental device [23] has been applied in Sentaurus process simulator [25]. From the process simulations the doping values and germanium concentration of the HBT are obtained. The doping profiles are plotted with two different epi layer doping as shown in Fig. 2. The device parameters obtained from the process simulations are tabulated in Table 1. The SOI HBT simulation results have been validated with the high speed experimental device [23] and the simulation results agree closely with

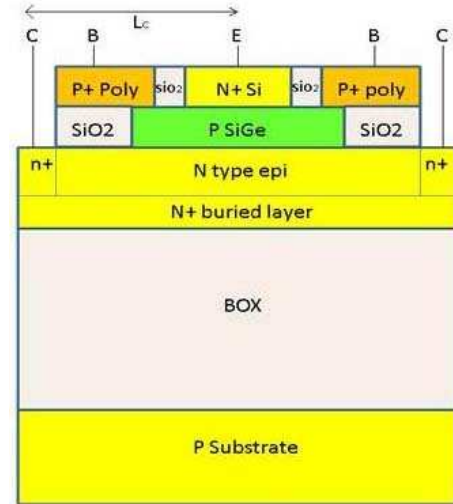


Fig. 1. Schematic of npn SOI HBT with n+ buried layer.

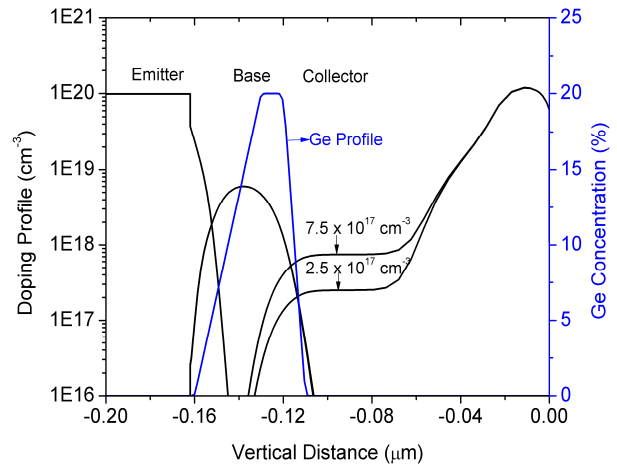


Fig. 2. Doping Profile and Ge profile of npn SOI HBT (epilayer thickness = 100 nm and buried layer thickness = 20 nm).

Table 1. SiGe HBT parameters

Parameter	Values	units
Emitter thickness	100	nm
Emitter Width	150	nm
Base thickness	30	nm
Buried layer	20	nm
Deposited epi layer	100	nm
BOX thickness	100	nm
Emitter doping	$1 \times 10^{20}$	$\text{cm}^{-3}$
Base doping	$1 \times 10^{19}$	$\text{cm}^{-3}$
Epi layer doping	$7.5 \times 10^{17}$	$\text{cm}^{-3}$
Buried layer doping	$1 \times 10^{20}$	$\text{cm}^{-3}$
Substrate doping	$1 \times 10^{15}$	$\text{cm}^{-3}$

the experimental findings. The experimental HBT uses SiGeC in the base layer. In our simulations, SiGe base layer has been used. The beta value of the experimental

device is nearly 1000. For our simulated device, the beta value is nearly 850. The peak  $f_t$  and  $BV_{CEO}$  values of the experimental device are 102 GHz and 1.8 V respectively. The peak  $f_t$  and  $BV_{CEO}$  values of the simulated HBT are 113 GHz and 1.78 V respectively. For this work, the collector profile has been engineered with a n+ buried layer and a deposited epi layer. For obtaining better  $f_t$  value a modified trapezoid Ge profile (0 % - 20 %) has been used. The slow grading of this profile minimizes the base-emitter capacitance compared to the device with steeper Ge grading profile. The 2D numerical simulations have been performed in the Sentaurus device simulator [26] to obtain the current density of npn SOI HBT. The models and the model parameters that have been used in the simulation are discussed in [18] and are as follows. The hydrodynamic model has been used in the simulation. The Slotboom bandgap narrowing model [27] is used to estimate the carrier density. Philips unified mobility model [28] has been chosen. In the recombination, Shockley-Read-Hall and Auger recombination model is used. The Okuto-Crowell model [29] is used to incorporate the impact ionization.

### III. OPTIMIZATION OF EPI LAYER DOPING IN SOI HBT

In the npn SOI HBT simulation study, a 1.2 V of  $V_{CE}$  is used and  $V_{BE}$  is varied from 0 V to 1.2 V. From Table 1, the epi layer doping value is varied and the other parameters are kept constant. This parameter is chosen to change the base collector space charge region inside the device. In the simulation the biasing scheme is forced- $V_{BE}$ . From the simulations, the base and collector currents have been obtained. The beta values are extracted as shown in Fig. 3. The small signal ac analysis has been performed to obtain the Y parameters. From the Y parameters the ac voltage gain ( $Y_{21}/Y_{22}$ ) is evaluated. The results are reported in Fig. 4. At low value of epi layer doping, the collector base space charge region is entirely towards collector side. Also the SOI HBT with low value of epi layer doping, the effective base layer thickness increases (in Fig. 2) which is the cause of improved output impedance. At low and moderate injection, the ac voltage gain increases by decreasing the epi layer doping. This is due to dominant contribution of  $R_C$  in the  $r_0 \parallel R_C$  value. At low and moderate injection,

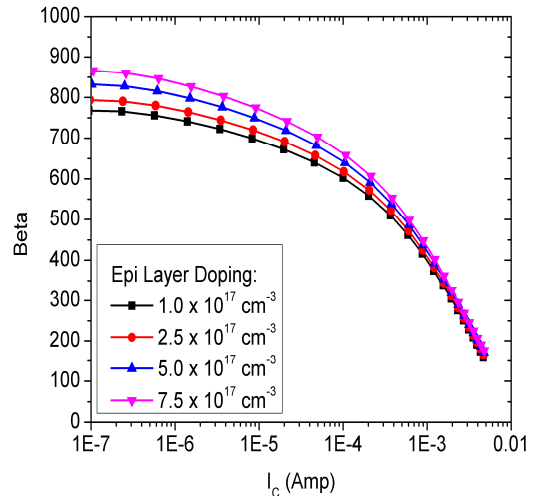


Fig. 3. Beta of npn SOI HBT with different epi layer doping.

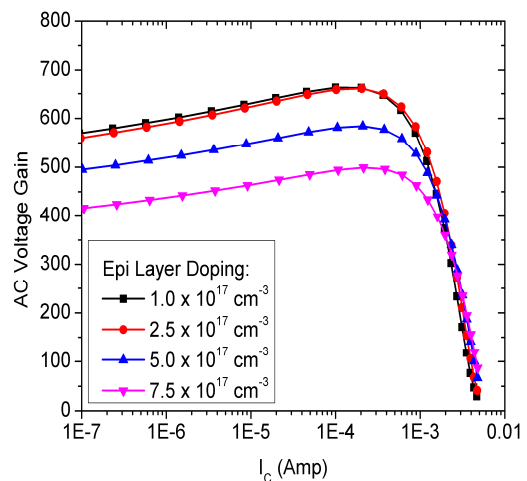


Fig. 4. AC Voltage gain of npn SOI HBT with different epi layer doping.

the  $r_0$  value is much higher than the  $R_C$ . However, at high injection, the  $r_0$  value is a dominant factor in the ac voltage gain. Therefore, at ( $I_C > 1$  mA), the HBT with high value of epi layer doping has high ac voltage gain.

Fig. 5 shows the unity current gain frequency of HBT. The HBT with high epi layer doping offers better  $f_t$  value. This is due to delayed saturation of collector current. The base-collector space charge region expands towards collector side vertically because the depletion width towards collector side is approximately 60 nm for the HBT with  $7.5 \times 10^{17} \text{ cm}^{-3}$ . In the calculation 1.2 V of reverse bias was used. The actual deposited epi layer thickness is 100 nm. But due to the diffusion buried layer, the effective epi layer thickness has become nearly 70 nm. When epi layer doping value decreases, the space charge region expands

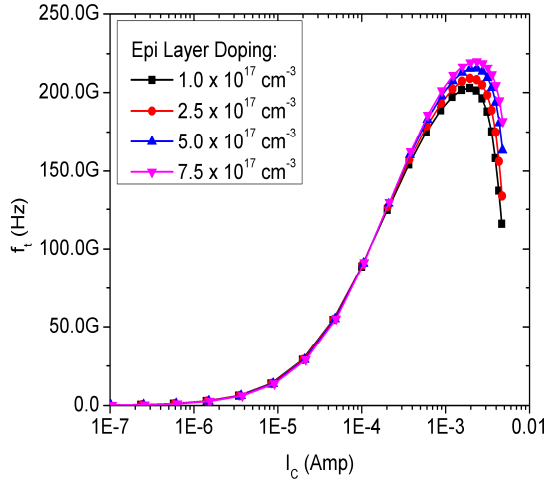


Fig. 5.  $f_t$  of npn SOI HBT with different epi layer doping.

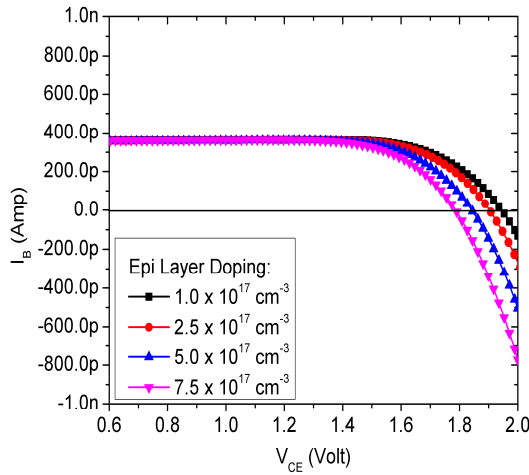


Fig. 6.  $BV_{CEO}$  of npn SOI HBT with different epi layer doping.

Table 2. Performance comparison of SOI HBT with different epi layer doping values

Epi Layer Doping ( $\text{cm}^{-3}$ )	Peak $f_t$ (GHz)	$BV_{CEO}$ (Volt)	$f_tBV_{CEO}$ Product (GHzV)
$1.0 \times 10^{17}$	202.9	1.94	393.6
$2.5 \times 10^{17}$	208.9	1.90	397.0
$5.0 \times 10^{17}$	215.3	1.84	396.1
$7.5 \times 10^{17}$	220.1	1.78	391.7

laterally towards collector contacts.

The base current reversal effect in bipolar transistor is discussed in [30]. In the simulation, the breakdown voltage is obtained from the base current reversal point for  $V_{BE} = 0.7$  V. The results are reported in Fig. 6. From Table 2, it has been observed that the  $f_t$  value decreases and the  $BV_{CEO}$  value increases by decreasing the epi layer doping. The increase in  $BV_{CEO}$  value is due to the

lateral expansion of space charge region. The trade off suggests that there is an optimal doping value that would be necessary to maximize the  $f_tBV_{CEO}$  product. As shown in [31, 32], there is a tradeoff between  $f_t$  and  $BV_{CEO}$  in the bipolar transistor design. In our simulation we analyzed the tradeoff and the  $f_tBV_{CEO}$  product. The  $f_tBV_{CEO}$  product has been obtained for different doping levels of the epi layer. From the results reported in Table 2, it has been observed that the SOI HBT with  $2.5 \times 10^{17} \text{ cm}^{-3}$  epi layer doping has highest  $f_tBV_{CEO}$  product (397 GHzV). The  $f_tBV_{CEO}$  tradeoff suggests that the device performance can be improved in two ways. In the first approach, the supply voltage could be increased to achieve the high  $f_t$  value and in the second approach, the film thickness could be scaled to achieve similar improvement.

In both approaches, the Kirk current of the SOI HBT is improved. The details are discussed in the subsequent section. In both ways, power consumption of the HBT would increase as discussed below. The  $f_t$  value has been obtained by raising the supply voltage as shown in Fig. 7. At high supply voltage ( $V_{CE}=1.8$  V), the collector base reverse bias of the HBT increases. With increased reverse bias, the depletion width of collector-base diode is increasing to compensate the reduced amount of charges. Therefore, the reverse biased collector-base capacitance value decreases by applying high supply voltage. At peak  $f_t$  ( $V_{BE} = 1.032$  V), the  $(C_{BE}+C_{BC})$  of the SOI HBT is 12.23 fF for 1.2 V of  $V_{CE}$ . Due to the aforementioned reason, this capacitance value decreases to 11.1 fF by applying 1.8 V of  $V_{CE}$ . Additionally, the peak  $f_t$  value of the SOI HBT ( $V_{CE} = 1.8$  V) is obtained at high collector current compared to the HBT with 1.2 V of  $V_{CE}$ . This is because the increase in the trans-conductance value is significant compared to the increase in the capacitance value at  $V_{BE} = 1.032$  V (corresponding to peak  $f_t$ ) and hence the peak  $f_t$  value is obtained at the collector current of 3.58 mA. This delays the onset of the Kirk effect of the transistor. As can be seen from the Fig. 7, a maximum of 245 GHz of  $f_t$  value can be obtained by using 1.8 V of  $V_{CE}$  with an epi layer doping of  $2.5 \times 10^{17} \text{ cm}^{-3}$ . The Kirk current of the HBT [33] can be written as given in Eq. (1).

$$I_C, \text{Kirk} = qA_E v_{\text{sat}} N_C \left( 1 + \frac{2\mathcal{E}(V_{CB} + \phi_{bi})}{qN_C W_C^2} \right) \quad (1)$$

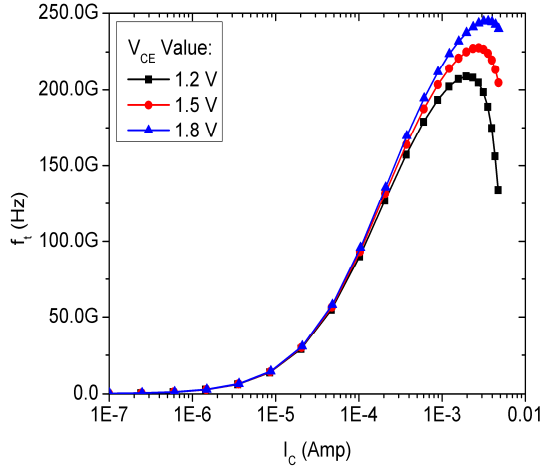


**Fig. 7.**  $f_t$  of npn SOI HBT with epi layer doping of  $2.5 \times 10^{17} \text{ cm}^{-3}$ .

where  $N_C$  is the the doping value of the deposited epi layer and  $W_C$  is the thickness of the layer.  $V_{CB}$  is the applied reverse bias voltage to the collector-base diode. The onset of Kirk current can be increased by increasing the epi layer doping, supply voltage and reducing the thickness of the epi layer. By increasing the Kirk current value, the charging time component of the transistor can be reduced. For the epi layer doping of  $2.5 \times 10^{17} \text{ cm}^{-3}$ , the  $BV_{CEO}$  of the SOI HBT is 1.9 V. This results in 465.5 GHzV of  $f_t BV_{CEO}$  product. The improved performance of the SOI HBT with n+ buried layer is obtained at the cost of power consumption. At peak  $f_t$ , the power consumption of this HBT with 1.2 V and 1.8 V  $V_{CE}$  are 2.33 mW and 6.4 mW respectively. At higher supply the HBT consumes more power and hence the self heating of the transistor is of major concern. Due to this, 100 nm BOX thickness has been used in this design so that thin BOX will compensate for the thermal performance due to high supply voltage. The research efforts are on towards thin BOX devices [34, 35] that would improve the self heating performance.

The detailed study of the electro thermal behavior of the HBT has been studied in ( $V_{CE}$ ,  $I_C$ ) plane [36]. In this simulation collector-emitter voltage is varied. Thermal resistances of three SOI HBTs with different geometries are reported in [37] with values 4430, 5850 and 6680 K/W. The results reported [37] suggests that the thermal performance can be made better for properly choosing the device geometry. 3D TCAD simulation with lattice temperature will be required for finding the optimal device geometry and heat flow mechanism inside the

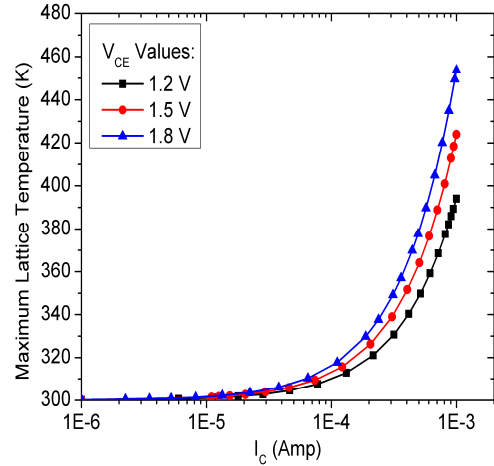


**Fig. 8.** Maximum lattice temperature of HBT with different  $V_{CE}$ .

device. In the 2D simulation study the geometry is limited by device width. Therefore, using 2D simulation, the geometry optimization cannot be done for finding the device structure for better thermal performance. A thermal resistance of  $4 \times 10^{-5} \text{ Kcm}^2/\text{W}$  has been used between the SOI HBT and the heat sink for the simulation. Heat equations have been solved by coupling the temperature. The model parameters for analyzing the self heating effect are discussed in [18]. In this work the same parameters have been used to estimate the maximum lattice temperature of the SOI HBT. The maximum lattice temperature of SOI HBT is shown in Fig. 8 with different voltages. A maximum of 408 K temperature is observed in the HBT with 1.8 V of supply voltage and 1 mA of collector current. This value is 42 K higher compared to the HBT with 1.2 V of  $V_{CE}$  at 1 mA of collector current.

#### IV. SCALING OF EPI LAYER THICKNESS OF SOI HBT

As the  $f_t BV_{CEO}$  product of the HBT is better with an epi layer doping value of  $2.5 \times 10^{17} \text{ cm}^{-3}$ , this value has been used and the epi layer thickness has been scaled to study the HBT performance. The  $V_{CE}$  value is kept 1.2 V and  $V_{BE}$  is varied from 0 V to 1.2 V. The small signal analysis of the SOI HBT has been performed to obtain the ac voltage gain with different epi layer thicknesses. The voltage gains are compared and plotted as shown in Fig. 9. The results show that the voltage gain decreases as the epi layer thickness of the HBT decreases. This

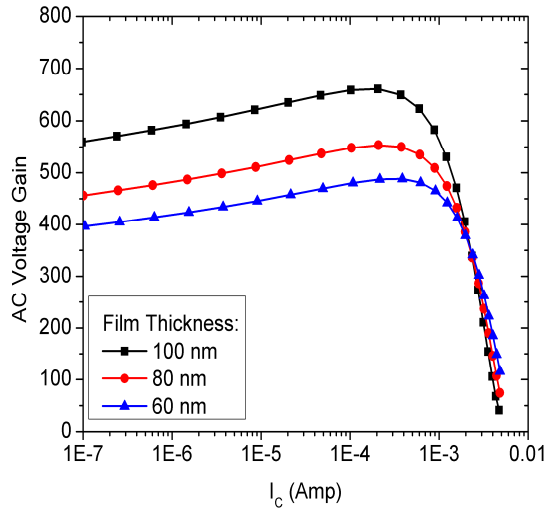


**Fig. 9.** AC Voltage gain of HBT. Epi Layer doping= $2.5 \times 10^{17} \text{ cm}^{-3}$  and the epi layer thickness is varied

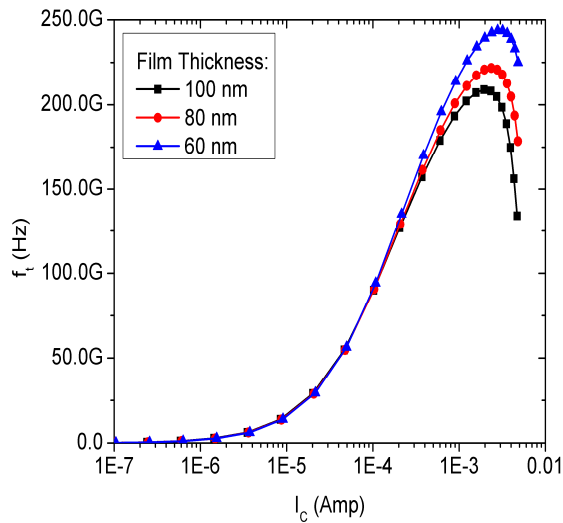


**Fig. 10.**  $f_t$  of SOI HBT. Epi Layer doping= $2.5 \times 10^{17} \text{ cm}^{-3}$  and the epi layer thickness is varied

reduction in voltage gain is due to the reduction in the output impedance resulting from the reduction in base-collector space charge region and the diffusion of dopants from the buried layer towards base side. The  $f_t$  values are plotted in Fig. 10 with different epi layer thickness values. The diffusion of dopants from the buried layer shows that the epi layer thickness can be scaled upto 60 nm. The onset of the Kirk current increases with the scaling of the epi layer thickness as discussed in the Eq. (1). Thus the device performance can be improved in terms of speed by scaling the epi

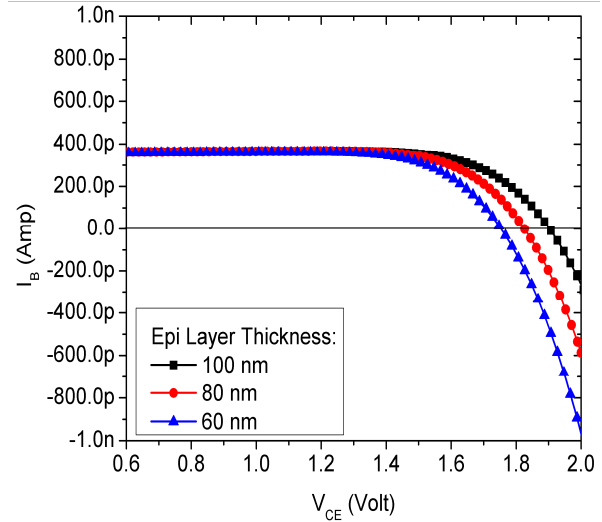


**Fig. 11.**  $BV_{CEO}$  of HBT. Epi Layer doping= $2.5 \times 10^{17} \text{ cm}^{-3}$  and the epi layer thickness is varied

**Table 3.** Performance comparison of HBT by varying epi layer thickness

Epi Layer Thickness (nm)	Peak $f_t$ (GHz)	$BV_{CEO}$ (Volt)	$f_t BV_{CEO}$ Product (GHzV)	Power (mW)
100	208.9	1.975	358.4	2.33
80	221.7	1.842	367.3	2.84
60	243.9	1.75	426.8	3.35

layer thickness. The breakdown voltage of SOI HBT has been measured from base current reversal point at  $V_{BE}=0.7 \text{ V}$  with different epi layer thicknesses. The results are plotted as shown in Fig. 11. As can be seen the high  $f_t$  value can be obtained at the cost of the breakdown voltage of the device. However, the breakdown voltage of 1.75 V is nominal for the transistor to be operated with 1.2 V of  $V_{CE}$ . The summary of the performance is given in Table 3.

By scaling the epi layer thickness of the HBT, high  $f_t BV_{CEO}$  product can be obtained. From the results it can be found that the HBT with 20 nm buried layer and 60 nm epi layer has a maximum of 243.9 GHz  $f_t$  value and 1.75 V of  $BV_{CEO}$  value resulting in 426.8 GHzV  $f_t BV_{CEO}$  product. This performance has been achieved at 3.35 mW of power consumption. The power consumption can be minimized by lowering the collector current instead of operating the HBT at its peak  $f_t$  value.

The simulation results suggest that the HBT with low epi layer thickness value would provide low power solution with reasonable performance. The  $f_t BV_{CEO}$

product can be improved by increasing the base current in SiGe HBTs with a SiGe spike inside the emitter [38]. This technique would provide low current gain value as discussed in the paper. The physical and electrical performance limits of the HBT have been predicted in [39, 40]. In this work, process and device cosimulations have been performed so that high performance SOI BiCMOS technology could materialize. The HBT with thick buried layer would provide better performance. However, compatibility with fully depleted SOI CMOS will be a challenge because in advanced fully depleted SOI CMOS technology, the film thickness is very low. The addition of this HBT to fully depleted SOI CMOS technology would provide high performance SOI BiCMOS technology.

Also, the HBT with buried nickel silicide layer is investigated. The simulation studies show that the HBT with nickel silicide buried layer has less diffusion towards the epi layer. Due to this, the film thickness could be scaled up to 40 nm to reduce the collector transit time. In this case, the effective epi layer thickness is around 20 nm due to the diffusion from the buried silicide layer. Using 40 nm epi layer and 20 nm buried layer the  $f_t$  value of the HBT is 273 GHz. Although the performance is better in case of HBT with buried silicide layer, integrating the SOI HBT with buried silicide layer to the fully depleted SOI CMOS would be a challenge. There are process issues while integrating with SOI CMOS.

The benefits of designing analog/RF systems with HBTs and digital systems with CMOS are discussed in [41]. Similar benefits can be found using this technology particularly for highly integrated mixed signal chips. Thus, RF circuits and systems can be designed for 60 GHz short range communication and 77 GHz automotive radar applications [42] with better performance and low noise figure.

## V. CONCLUSION

The simulation study of npn SOI HBT with buried layer has been performed with trapezoidal Ge profile. The epi layer doping is varied to vary the base collector space charge region inside the device and the tradeoff in the HBT performance is studied in terms of DC current gain, AC voltage gain, unity current gain frequency and

breakdown voltage. From the results it is observed that a maximum of 397 GHzV  $f_tBV_{CE0}$  product can be obtained with  $2.5 \times 10^{17} \text{ cm}^{-3}$  epi layer doping using  $V_{CE}$  of 1.2 V. As the breakdown voltage is higher at low value of epi layer doping, the supply voltage can be raised up to 1.8 V so that the  $f_tBV_{CE0}$  product can be improved to 465 GHzV. The lattice temperature of the HBT has been studied at different supply voltages. At 1 mA collector current, the maximum lattice temperature of the HBT is 42 K higher while applying  $V_{CE}$  of 1.8 V in comparison to the HBT at the  $V_{CE}$  of 1.2 V. The epi layer film thickness is scaled to obtain the DC and AC characteristics of the npn SOI HBT. The  $f_tBV_{CE0}$  product of the HBT has been evaluated. With 60 nm epi layer thickness and 20 nm buried layer, the  $f_tBV_{CE0}$  product of the SOI HBT is 426 GHzV using 1.2 V of  $V_{CE}$ . This HBT can be used in high performance RF circuits and systems at 60 GHz and 77 GHz applications.

## REFERENCES

- [1] John D. Cressler, "SiGe HBT Technology: A New Contender for Si-Based RF and Microwave Circuit Applications," IEEE Transactions on microwave theory and techniques, vol. 46, no. 5, pp. 572–589, May 1998.
- [2] D. L. Harame, J. H. Comfort, J. D. Cressler, E. F. Crabbe, J. Y.-C. Sun, B. S. Meyerson, and T. Tice, "Si/SiGe Epitaxial-Base Transistors-Part I: Materials, Physics, and Circuits," IEEE Transactions on Electron Devices, Vol. 42, No. 3, pp. 455-468, March 1995.
- [3] D. L. Harame, J. H. Comfort, J. D. Cressler, E. F. Crabbe, J. Y.-C. Sun, B. S. Meyerson, and T. Tice, "Si/SiGe Epitaxial-Base Transistors-Part II: Process Integration and Analog Applications," IEEE Transactions on Electron Devices, Vol. 42, No. 3, pp. 469-482, March 1995.
- [4] S C Jain, S Decoutere, M Willander and H E Maes, "SiGe HBTs for application in BiCMOS technology: I. Stability, reliability and material parameters," Semiconductor Science Technology 16, R51–R65, 2001.
- [5] S C Jain, S Decoutere, M Willander and H E Maes, "SiGe HBT for application in BiCMOS technology: II. Design, technology and

- performance,” *Semiconductor Science Technology*, 16, R67–R85, 2001.
- [6] Katsuyoshi Washio, “SiGe HBT and BiCMOS technologies for optical transmission and wireless communication systems”, *IEEE transactions on electron devices*, Vol. 50, No. 3, pp. 656-668, March 2003.
- [7] Macro Racanelli and Paul Kempf, “SiGe BiCMOS technology for RF circuit applications,” *IEEE transactions on electron devices*, Vol. 52, No. 7, pp. 1259-1270, July 2005.
- [8] Grégory Avenier, Malick Diop, Pascal Chevalier, Germaine Troillard, Nicolas Loubet, Julien Bouvier, Linda Depoyan, Nicolas Derrier, Michel Buczko, Cédric Leyris, Samuel Boret, Sébastien Montusclat, Alain Margain, Sébastien Pruvost, Sean T. Nicolson, Kenneth H. K. Yau, Nathalie Revil, Daniel Gloria, Didier Dutartre, Sorin P. Voinigescu, and Alain Chantre, “0.13 μm SiGe BiCMOS Technology Fully Dedicated to mm-Wave Applications,” *IEEE journal of solid-state circuits*, vol. 44, no. 9, September 2009, pp. 2312 - 2321.
- [9] L. Boissonnet, F. Judong, B. Vandelle, L. Rubaldo, P. Bouillon, D. Dutartre, A. Perrotin, G. Avenier, P. Chevalier, A. Chantre and B. Rauber, “A 0.13 μm thin SOI CMOS technology with low-cost SiGe:C HBTs and complementary high-voltage LDMOS,” *Bipolar/BiCMOS Circuits and Technology Meeting*, 2006, pp. 1-4.
- [10] H. Rucker, B. Heinemann, R. Barth, D. Bolze, J. Drews, O. Fursenko, T. Grabolla, U. Haak, W. Hoppner, D. Knoll, S. Marschmeyer, N. Mohapatra, H. H. Richter, P. Schley, D. Schmidt, B. Tillack, G. Weidner, D. Wolansky, H.-E. Wulf, and Y. Yamamoto, “Integration of High-Performance SiGe:C HBTs with Thin-Film SOI CMOS,” *IEEE International Electron Devices Meeting*, 2004, pp. 239 – 242.
- [11] Jin Cai and Tak H. Ning, “Bipolar Transistors on Thin SOI: Concept, Status and Prospect,” *7<sup>th</sup> International Conference on Solid-State and Integrated Circuits Technology*, 2004, Proceedings, pp.2012-2107.
- [12] P. Chevalier, D. Lagarde, G. Avenier, T. Schwartzmann, B. Barbalat, D. Lenoble, J. Bustos, F. Pourchon, F. Saguin, B. Vandelle, L. Rubaldo, A. Chantre, “Low-Cost Self-Aligned SiGeC HBT Module for High-Performance Bulk and SOI RFCMOS Platforms,” *IEEE International Electron Devices Meeting*, 2005, pp. 963 – 966.
- [13] Jin Cai, Mahender Kumar, Michael Steigenvaldt, Herbert Ho, Kathryn Schonenberg, Kenneth Stein, Huajie Chen, Keith Jenkins, Qiqing Ouyang, Philip Oldiges, and Tak Ning, “Vertical SiGe-base Bipolar Transistors on CMOS-Compatible SOI Substrate,” *Bipolar/BiCMOS Circuits and Technology Meeting 2003*, pp. 215-218.
- [14] T.H. Ning, “Why BiCMOS and SOI BiCMOS,” *IBM Journal of Research and Development*, Volume: 46, Issue: 2.3, pp.181-186, 2002.
- [15] Mahender Kumar, Yue Tan and Johnny K. O. Sin, “A sample, high performance TF-SOI complementary BiCMOS technology for low power wireless applications” *IEEE Transactions on Electron Devices*, Vol. 49, No. 1, pp. 200-202, January 2002.
- [16] T. T. Tominari, M. Miura, H. Shimamoto, M. Arai, Y. Yoshida, H. Sato, T. Aoki, H. Nonamil, S. Wadal, H. Hosoel, K. Washio, and T. Hashimoto, “A 10 V complementary SiGe BiCMOS foundry process for high-speed and high-voltage analog applications” *BCTM 2007*, pp. 38-41.
- [17] Jeff A. Babcock, Greg Cestra, Wibo van Noort, Paul Allard, Scott Ruby, Jon Tao, Robert Malone, Alan Buchholz, Natasha Lavrovskaya, Wipawan Yindeepol, Craig Printy, Jamal Ramdani, Andre Labonte, Heather McCulloh, Yaojian Leng, Pat McCarthy, Don Getchell, Akshey Sehgal, Tracey Krakowski, Saurabh Desai, Chris Joyce, Peyman Hojabri, and Stefaan Decoutere, “CBC8: A 0.25 μm SiGe-CBiCMOS Technology Platform on Thick-Film SOI for High-Performance Analog and RF IC Design” *BCTM 2010*, pp. 41-44.
- [18] Prasanna Kumar Misra and S. Qureshi, “A Technique to Improve the Performance of an NPN HBT on thin film SOI,” *IEEE Journal of the Electron Devices Society*, Vol. 1, No. 4, April 2013, pp.92-98.
- [19] M. Bain, H. A. W. El Mubarek, J. M. Bonar, Y. Wang, O. Bui, H. Gamble, B. M. Armstrong, Peter L. F. Hemment, Steven Hall and Peter Ashburn, “SiGe HBTs on Bonded SOI Incorporating Buried Silicide Layers,” *IEEE Transactions on Electron Devices*, Vol. 52, No. 3,

- pp. 317-324, March 2005.
- [20] P. Chevalier, B. Barbalat, M. Laurens, B. Vandelle, L. Rubaldo, B. Geynet, S.P. Voinigescu, T.O. Dickson, N. Zerounian, S. Chouteau, D. Dutartre, A. Monroy, F. Aniel, G. Dambrine, and A. Chantre, "High-Speed SiGe BiCMOS Technologies:120-nm Status and End-of-Roadmap Challenges," Topical Meeting on Silicon Monolithic Integrated Circuits in RF Systems, 2007, pp. 18-23.
- [21] Benoit Barbalat, Thierry Schwartzmann, Pascal Chevalier, Benoit Vandelle, Laurent Rubaldo, Fabienne Saguin, Nicolas Zerounian, Frederic Aniel and Alain Chantre, "Carbon effect on neutral base recombination in high-speed SiGeC HBTs," Third International SiGe Technology and Device Meeting, 2006, pp. 1-2.
- [22] Carlos Mazure, Richard Ferrant, Bich-Yen Nguyen, Walter Schwarzenbach, Cecile Moulin, "FDSOI: From Substrate to Devices and Circuit Applications," ESSCIRC Sept. 2010, pp. 45-51.
- [23] Gregory Avenier, Pascal Chevalier, Benoit Vandelle, Damien Lenoble, Fabienne Saguin, Sebastien Fregonese, Thomas Zimmer, and Alain Chantre, "Investigation of fully- and partially-depleted self-aligned SiGeC HBTs on thin film SOI," Proceedings of ESSDERC, Grenoble, France, 2005, pp. 133-136.
- [24] T. Lacave, P. Chevalier, Y. Campidelli, M. Buczko, L. Depoyan, L. Berthier, G. Avenier, C. Gaquière, A. Chantre, "Vertical Profile Optimization for +400 GHz  $f_{MAX}$  Si/SiGe:C HBTs," Bipolar/BiCMOS Circuits and Technology Meeting (BCTM), 2010, pp. 49-52.
- [25] Sentaurus process user guide, Version G-2012.06, June 2012.
- [26] Sentaurus device user guide, Version G-2012.06, June 2012.
- [27] J. W. Slotboom and H. C. De Graaff, "Measurements of bandgap narrowing in Si bipolar transistors", Solid State Electronics 1976, Vol. 19, NO. 10, pp. 857-862.
- [28] D. B. M. Klaassen, "A Unified Mobility Model for Device Simulation—I. Model Equations and Concentration Dependence," Solid State Electronics 1992, Vol. 35, No. 7, pp. 953-959.
- [29] Y. Okuto and C. R. Crowell, "Threshold Energy Effect on Avalanche Breakdown Voltage in Semiconductor Junctions," Solid-State Electronics 1975, Vol. 18, No. 2, pp. 161-168.
- [30] Pong-Fei Lu and Tze-Chiang Chen, "Collector-base junction avalanche effects in advanced double-poly self-aligned bipolar transistors," IEEE Transactions on Electron Devices. Vol. 36. No 6. June 1989, pp.1182-1188.
- [31] E. O. Johnson, "Physical limitations on frequency and power parameters of transistors," IRE International Convention Record, pp. 27-34.
- [32] Kwok K. Ng, Michel R. Frei, and Clifford A. King, "Reevaluation of the  $f_tBV_{CEO}$  limit on Si Bipolar Transistors," IEEE Transactions on Electron Devices, vol. 45, no. 8, August 1998, pp. 1854-1855.
- [33] Alvin J. Joseph, John D. Cressler, David M. Richey, and Guofu Niu, "Optimization of SiGe HBT's for Operation at High Current Densities," IEEE Transactions On Electron Devices, Vol. 46, No. 7, July 1999, pp. 1347-1354.
- [34] Chang Woo Oh, Hyun Jun Bae, Jae Kyu Ha, Sang Jin Park, Bok Kyung Park, Dong-Won Kim, TaeYoung Chung, Kyung Seok Oh, and Won-Seong Lee, "A Novel Thin BOX SOI Technology Using Bulk Si Wafer for System-on-Chip (SOC) Application," Symposium on VLSI technology, 2009, pp. 96-97.
- [35] Siddharth Chouksey, Jerry G. Fossum and Shishir Agrawal, "Insights on design and scalability of Thin-BOX FD/SOI CMOS," IEEE transactions on electron devices, vol. 57, no. 9, september 2010, pp.2073-2079.
- [36] Niccolo Rinaldi and Vincenzo d'Alessandro, "Theory of Electrothermal Behavior of Bipolar Transistors: Part I—Single-Finger Devices," IEEE Transactions On Electron Devices, Vol. 52, No. 9, pp. 2009-2021, September 2005.
- [37] Alain Chantre, Gregory Avenier, Pascal Chevalier, Benoit Vandelle, Fabienne Saguin, Cristell Maneux, Didier Dutartre and Thomas Zimmer, "SiGe HBT design for CMOS compatible SOI," International SiGe Technology and Device Meeting, 2006, pp. 1-2.
- [38] L. J. Choi, S. Van Huylbroeck, A. Piontek, A. Sibaja-Hernandez, E. Kunnen, P. Meunier-Beillard, W. D. van Noort, E. Hijzen, and S. Decoutere, "On the Use of a SiGe Spike in the Emitter to Improve

the  $fT_x$  BVCEO Product of High-Speed SiGe HBTs," IEEE Electron Device Letters, Vol. 28, No. 4, April 2007, pp. 270-272.

- [39] Michael Schröter, Gerald Wedel, Bernd Heinemann, Christoph Jungemann, Julia Krause, Pascal Chevalier and Alain Chantre, "Physical and Electrical Performance Limits of High-Speed SiGeC HBTs—Part I: Vertical Scaling," IEEE Transactions on Electron Devices, Vol. 58, No. 11, november 2011, pp.3687-3696.
- [40] Michael Schröter, Julia Krause, Niccolò Rinaldi, Gerald Wedel, Bernd Heinemann, Pascal Chevalier, and Alain Chantre, "Physical and Electrical Performance Limits of High-Speed SiGeC HBTs—Part II: Lateral Scaling," IEEE Transactions on Electron Devices, Vol. 58, No. 11, November 2011, pp. 3697-3706.
- [41] John D. Cressler, "A Retrospective on the SiGe HBT: What We Do Know, What We Don't Know, and What We Would Like to Know Better," Silicon Monolithic Integrated Circuits in RF Systems (SiRF) 2013, pp. 81-83.
- [42] P. Chevalier, T.F. Meister, B. Heinemann, S. Van Huylenbroeck, W. Liebl, A. Fox, A. Sibaja-Hernandez and A. Chantre, "Towards THz SiGe HBTs," Bipolar/BiCMOS Circuits and Technology Meeting (BCTM), 2011, pp.57-65.



**Prasanna Kumar Misra** was born in Berhampur, India, in 1983. He received Bachelor's degree in Electronics and Instrumentation Engineering from National Institute of Science and Technology, Berhampur, India in 2005. From

2006 to 2007 he worked as project associate in the department of electrical engineering, IIT Kanpur and currently he is pursuing Ph.D in the department of Electrical Engineering at IIT Kanpur. His research interests are semiconductor device modeling, Analog/RF circuit design and mixed signal system design.



**S. Qureshi** (SM'94) received the B.E. degree from the University of Kashmir, Srinagar, India, in 1974 and the M.S. and Ph.D. degrees from the University of California, Berkeley, in 1986 and 1991, respectively. From 1975 to 1981, he was with the

Department of Atomic Energy, India, where he served as Scientific Engineer. Since 1992, he has been with the Indian Institute of Technology Kanpur, Kanpur, India, where he is currently a Professor in the Department of Electrical Engineering. His research interests include thin-film transistors, device physics and modeling, VLSI design, nuclear radiation detectors, and electronics. Dr. Qureshi is a Fellow of the Institution of Electronics and Telecommunication Engineers, India, and the Indian Association of Radiological Protection.